

Buffer medium exchange in continuous cell and particle streams using ultrasonic standing wave focusing

Per Augustsson · Lena B. Åberg ·
Ann-Margret K. Swärd-Nilsson · Thomas Laurell

Received: 27 April 2008 / Accepted: 1 July 2008 / Published online: 18 July 2008
© Springer-Verlag 2008

Abstract A microfluidic strategy to perform buffer exchange of particle and cell suspensions in a continuous flow format on chip is presented. Ultrasonic standing wave technology is utilized to confine particulate matter to the centre of a buffer exchange channel while particle free buffer is sequentially aspirated via capillaries that branch off from the buffer exchange channel. At each such branch, clean buffer is supplied at an equal flow-rate from a capillary at the opposing channel wall, generating a sideways translation of the original buffer, laminated with a wash buffer stream. Each such junction increases the buffer exchange ratio accordingly. The reported buffer exchange system provides means to adjust buffer exchange conditions on-line by tuning the ratio of the cross-flow wash buffer relative the sample suspension flow rate. The system performance was evaluated using 5 μm polystyrene microbeads and a dye as the model contaminant. Wash efficiencies up to 96.4% were accomplished with a 0.2% solid content bead suspension, using eight cross-flow junctions, effectively exchanging the carrier buffer twice. The corresponding data for erythrocyte washing was recorded to be 98.3% at a haematocrit of 2%.

Keywords Ultrasonic standing wave · Particle washing · Erythrocytes · Acoustic radiation force · Buffer medium exchange

P. Augustsson (✉) · T. Laurell
Division of Nanobiotechnology,
Department of Electrical Measurements, Lund University,
P.O. Box 118, 221 00 Lund, Sweden
e-mail: per.augustsson@elmat.lth.se

L. B. Åberg · A.-M. K. Swärd-Nilsson
Blood Centre Skåne, Lund University Hospital,
221 85 Lund, Sweden

Introduction

Buffer medium exchange in cell biology and in clinical practice is widely employed utilizing centrifugation principles where the cells undergo high mechanical stress, being pelleted by the centrifugation process and subsequently resuspended in solution [1]. In bioanalytical processes biospecific microbeads and chromatographic material is frequently used for sample decomplexing by affinity purification on solid microbead surfaces [2]. Standard protocols for bead based assays are widely used and commonly include a wealth of buffer exchange procedures before obtaining the final readout [3].

In line with the continuous development of integrated miniaturized bioanalytical systems on a chip [4], buffer unit operations for cell and particle suspensions become a major challenge since centrifugation principles to a large extent are no longer applicable in the microchip domain. Key strategies to overcome this hurdle are currently focusing on the use of externally induced physical forces on particles and cells in the microfluidic domain of the chip. These can thus be translated into a flow path which holds a new buffer precisely defined by laminar flow conditions [5]. Systems based on optical forces such as laser tweezers [6] or optical lattices [7] have been utilized to spatially control localization of cells and microbeads in microenvironments and is a standard technology these days. A most widely used approach employs dielectrophoretic forces [8, 9] to drive particulate matter into defined regions within a microfluidic stream and thus enabling chip integrated buffer exchange conditions. In order to become less dependent of the liquid carrier composition e.g. in terms of ionic strength, magnetic microbeads and magnetophoresis [10] have emerged as a promising approach to accomplish on-chip buffer exchange operations. Recently, hydrodynamic filtration has been

demonstrated as a potential cell handling technique for buffer exchange [11, 12]. The buffer exchange was realized in a cross-flow configuration similar to what is outlined in this paper, however the particle/cell retention mechanism is substantially different.

Recent developments now also propose the use of acoustic standing wave fields (acoustophoresis) to spatially manipulate particles and cells in microfluidic systems [13, 14]. Acoustophoresis has proven to be a robust method to perform buffer exchange operations in microfluidic systems. Along this line Harris et al. [15] outlined a silicon glass microfabricated device for particle translation and Hawkes et al. demonstrated a quartz glass/PDMS micro-device in which yeast cells were washed in a continuous flow format [16] for the first time. In 2005 Petersson et al. [17] proposed an optional solution, The Lund method, [18] to buffer medium exchange using ultrasonic standing waves, which enabled optical surveillance of the continuous buffer exchange process.

This paper describes an alternative method to accomplish buffer exchange sequences for particle and cell suspensions on-chip. Rather than performing a single translation of the particulate matter into a new flow path as in [17], the particles are maintained in a focused stream in the middle of a flow channel by means of an ultrasonic standing wave, while the carrier buffer is sequentially exchanged via lateral flow streams. The wash conditions can thus be tuned either by the magnitude of the cross-flow or by incorporating an increased number of cross-flow streams along the buffer exchange channel.

Theory

Acoustic radiation force

The primary acoustic radiation force, Eq. 1, on a compressible spherical particle in a plane standing pressure field [19, 20], is commonly the dominating driving force in acoustic standing wave particle manipulation with particle sizes above approximately 1 μm diameter [21, 22].

$$F_r = -\left(\frac{p_0^2 V_p \beta_m \pi}{2\lambda}\right) \phi(\beta, \rho) \sin\left(\frac{4\pi x}{\lambda}\right) \quad (1)$$

where

$$\phi = \frac{5\rho_p - 2\rho_m}{2\rho_p + \rho_m} - \frac{\beta_p}{\beta_m} \quad (2)$$

The parameters of Eqs. 1 and 2 have the following notation:

p_0 pressure amplitude
 λ ultrasonic wavelength

x distance from a pressure node in the direction of the wave
 V_p particle volume
 β_m compressibility of the suspending medium
 β_p compressibility of the particle
 ρ_m density of the suspending medium
 ρ_p density of the particle

Even though it has yet to be experimentally verified that Eqs. 1 and 2 are in all parts valid for the acoustic chamber that is presented in this paper, previous work has shown that particles in microfluidic systems can be translated relative to a surrounding liquid phase if the acoustic contrast factor (ϕ -factor) is non zero [14, 23]. If the ϕ -factor is positive i.e. if the particle is dense and/or less compressible compared to the liquid phase it will move towards the nearest nodal position, while it will move towards the nearest antinode for negative ϕ -factors [24].

For low Reynolds' numbers the velocity of a particle in the pressure field is mainly determined by the primary acoustic radiation force and the counteracting Stokes' drag force [25],

$$F_r(x) = 3\pi\eta d v(x) \quad (3)$$

where η (Pa s) denotes the viscosity of the medium, d is the diameter of the particle and v is the velocity of the particle relative to the medium. Since F_r is proportional to the volume of the particle and consequently to the cube of the diameter, one can (after rearrangement of Eq. 3) assert that the velocity of a particle under influence of the primary acoustic radiation force is proportional to the square of the diameter.

$$v(x) \propto d^2 \quad (4)$$

This explains why a larger particle will move faster than a smaller one in a standing wave field, given that they have the same acoustic properties. Acoustic size separation of particles in a continuous flow format has previously been reported by Kapishnikov et al. [26] and Petersson et al. [27].

Experimental

Chip manufacturing

A micro channel structure was wet etched in a Silicon wafer (<110>, 3 in., 375 μm thick) using standard UV-lithography and KOH protocols. The structure consisted of a 6 cm long main channel (width 375 μm , height 150 μm) intersected by eight narrow (~ 150 μm) channel segments forming cross-flow junctions along the structure. All sections of the structure are aligned perpendicular to the (111)-planes in the crystal structure in order to achieve flat parallel walls as

well as high aspect ratio in the side inlets and outlets. Borosilica glass (1.1×18×70 mm; Glasteknik i Emmaboda AB, Emmaboda, Sweden, <http://www.glasteknik.nu/>) with drilled holes for the fluid connections was anodically bonded to the silicon chip to seal the channel structure. Silicone tubing (i.d. 1 mm; Rausil FG, Rehau AB, Örebro, Sweden, <http://www.rehau.se/>) was glued over the holes for easy connection to the external TFE teflon tubing (i.d. 0.5 mm; 58697-U, Supelco, Bellefonte, PA, http://www.sigmaaldrich.com/Brands/Supelco_Home.html; Fig. 1).

Ultrasonic actuation

For actuation of the ultrasound a 9 by 6 mm piezoceramic crystal (Pz26, Ferroperm Piezoceramics AS, Kvistgard, Denmark, <http://www.ferroperm-piezo.com/>) resonant at ~2 MHz, was glued (Loctite 3430, Henkel Loctite Corporation, Helsinki, Finland, <http://www.loctite.com/>) to one corner of the glass lid (Fig. 1). The 2 MHz vibrations match a $\lambda/2$ resonance criterion in the 375- μm wide channel to produce a standing pressure field, having a pressure node along the centre of the main channel flow. A function generator (HP 3325B, Hewlett-Packard Inc., Palo Alto, CA, USA) and a power amplifier (AG 1020, T&C Power conversion inc., Rochester, NY, USA, <http://www.tcpowerconversion.com/>) were used for driving the transducer with a sinusoidal continuous wave. The voltage over the transducer was monitored by an oscilloscope (TDS 1002, Tektronix UK Ltd., Bracknell, UK, <http://www.tek.com/>) and a watt meter (43 Thruline Wattmeter, Bird Electronic Corp., Cleveland, OH, USA, <http://www.bird-electronic.com/>) and adjusted to 25 V_{pp} delivering 0.6 W net power to the piezoceramic transducer in all of the presented experiments. The temperature on the chip surface was approximately 30 °C measured at the vicinity of the piezoceramic transducer using a Pt100-sensor.

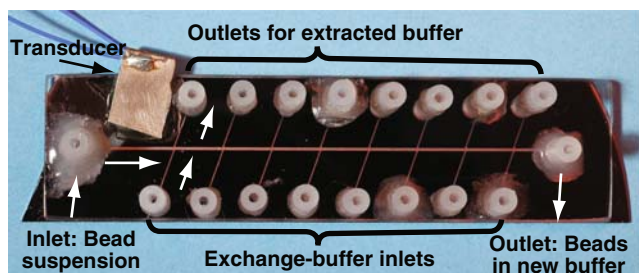


Fig. 1 Photo of the buffer exchange chip with the glued piezoceramic transducer positioned near the pre focusing segment. Pieces of silicone tubing are glued on top of the fluid in and outlets for connections of external tubing. Beads or cells are acoustically focused towards the centre of the flow throughout the horizontally oriented main channel

Flow-system setup

Bead or cell suspensions were infused into the chip at flow rates of 50–120 $\mu\text{L min}^{-1}$ from a 10 mL glass syringe (1010 TLL, Hamilton Bonaduz AG, Bonaduz, Switzerland, <http://www.hamiltoncompany.com/>) mounted in a syringe pump (NE1000, New era pump systems inc., Farmingdale, NY, USA, <http://www.syringepump.com/>). Sedimentation of the beads and cells in the syringe was prevented using an in house devised syringe mixer. Wash fluids were supplied to the chip via 8 plastic syringes (1 mL; BD Plastipak, Becton Dickinson S.A., Madrid, Spain) mounted in parallel in a modified syringe pump (WPI sp210iwz, World Precision Instruments Inc., Sarasota, FL, USA, <http://www.wpiinc.com/>). Waste fluids were collected into eight syringes mounted onto that same syringe pump in the opposite direction. The wash fluid flow rate was adjusted between 25–40% of the sample infusion flow rate (Fig. 2).

Sample preparation

Two bead mixtures containing blue dye were prepared accordingly; Doppler fluid for flow Doppler phantoms (Dansk Fantom Service, Jyllinge, Denmark, <http://www.fantom.suite.dk/>) was diluted in Milli Q water to a final content of orgasol polyamide particles (~5 μm diameter), Triton X-100 (0.2%), NaEDTA (0.02%), sodium benzoate (0.02%) and citric acid (0.002%). Evans blue (EB; 200 $\mu\text{g mL}^{-1}$; Merck, Darmstadt, Germany, <http://www.merck.de/>) was added to the suspension as a model contaminant. The bead content of the mixtures was ~2 vol.% (~500×10⁶ mL⁻¹) and ~0.2 vol.% (~50×10⁶ mL⁻¹), respectively. A washing buffer solution was also prepared containing Triton X-100 (0.2%; Prolabo #28 817.295, Paris, France,

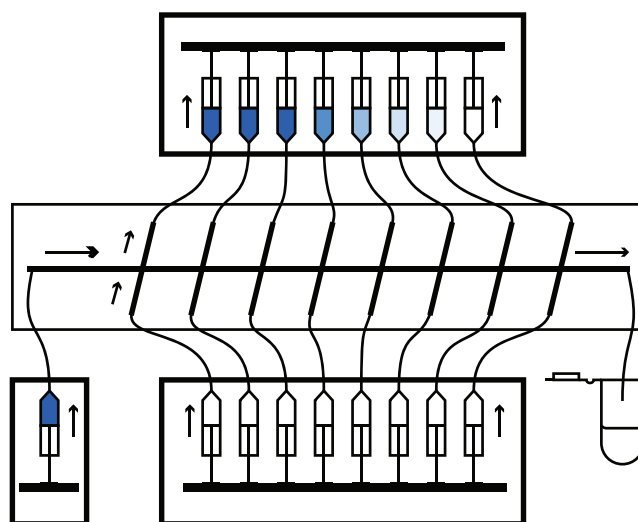


Fig. 2 Schematic of the external flow setup

<http://www.vwr.com/>) and EDTA (0.02%; Pro analysi, Merck, Darmstadt, Germany) in MilliQ.

A mixture containing red blood cells and blue dye was prepared by dilution and washing of whole blood two times in a buffer containing PBS (0.01 M, pH 7.4) and EB (0.02%w). The haematocrit of the mixture was ~2% measured by centrifugation (Haematokrit 210, Hettich Zentrifugen, Tuttlingen, Germany).

Analysis of washing performance

Surveillance of the process was performed by manual visual inspection using a boom stand microscope (SMZ-2T, Nikon, Tokyo, Japan) positioned above the chip. Photos were taken with a standard digital c-mount camera. All bead and cell mixtures were analyzed regarding particle number concentration and EB content before and after passing through the chip. A Coulter counter (Multisizer 3, Beckman Coulter Inc., Fullerton, CA, USA, <http://www.beckmancoulter.com/>) was used for retrieving the size distribution of particles from which the number of particles per milliliter and the particle volume fraction could be calculated by summing all size bins from 2 to 8 μm for beads and from 4 to 10 μm for RB cells. EB content in the supernatant of the samples was measured by absorption measurements at 595 nm in a micro plate spectrophotometer (Multiskan Multisoft, Labsystems, Helsinki, Finland). Recovery of beads/cells and transfer of dye through the device were calculated as the percentage of the measured output concentration relative to the input concentration.

Results

Microfluidic buffer exchange principle

The particle suspension was injected through an 11-mm long acoustically active pre focusing segment of the main channel that translated beads or cells towards the centre of the flow in a narrow band (Fig. 3), prior to reaching the first flow junction. At the first cross-flow junction a defined fraction of the main channel flow (25–40%), is aspirated (side shifted) from one side outlet of the channel while the same amount of fresh wash buffer is infused via the opposing inlet. Since the particles are confined in a fine band in the channel centre they will remain in the main channel while the specified fraction of the carrier buffer is extracted through the side outlet. The band of particles will, however, display a shift towards the side outlet positioning them closer to the side wall of the main channel. When propagating along the main channel, after the first buffer extraction junction, the band of particles will continue to experience an acoustic standing wave force and will again be focused in the centre of the flow, along the 6-mm long segment, preceding the following buffer exchange junction. When reaching the subsequent cross-flow junction the process of exchanging the carrier buffer is repeated. In theory an exchange rate of 25% in four consecutive flow junctions would accomplish a complete buffer exchange in a particle suspension, not accounting for diffusion based, bead associated or acoustic carry over of dissolved species. By increasing the relative exchange rate of each junction

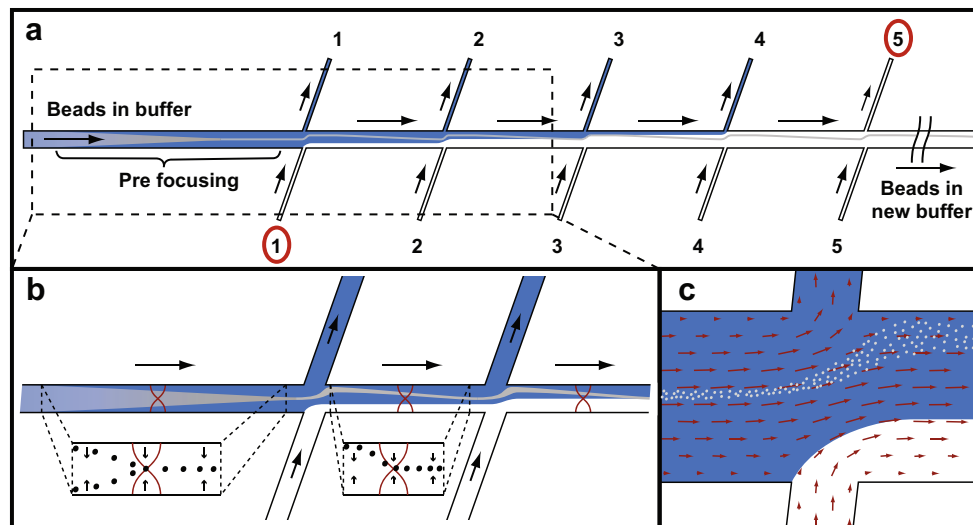


Fig. 3 Schematic of the acoustic washing device showing **a** the pre-focusing segment and the first five buffer exchange junctions. In the first four junctions the original buffer (*dark*) is extracted on the upper side of the main channel while new colourless buffer is added on the lower side. Since each junction has an exchange rate of 25% of the main flow, the buffer injected at inlet 1 will end up in outlet 5.

b The acoustic pressure field will exert a force on the particles towards the centre of the channel throughout the device, repeatedly preventing them from being extracted through the side outlets. **c** When the band of particles reaches a flow junction it will follow the side-shift in the flow rather than remaining in the centre of the channel

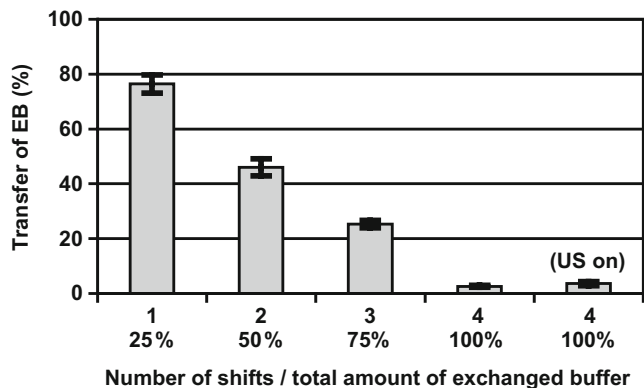


Fig. 4 Histogram showing the transfer of EB in a particle-free system when exchanging 25% to 100% of the $80 \mu\text{L min}^{-1}$ main channel volume flow in 1 to 4 sequential cross-flow junctions

and/or the number of active junctions, the total amount of exchanged medium can easily be increased to over 200% in the demonstrated eight junction chip, providing means of tuning the wash efficiency on-line over a wide range. A typical main channel average flow rate of $80 \mu\text{L min}^{-1}$ yields an average particle retention time in the channel of 2.5 s for randomly distributed particles. Since the particles are acoustically focused to the centre of the flow profile the stipulated retention time is slightly overestimated. The total time scale of the buffer exchange process would thus last 12.5 min for a 1-mL bead suspension with an approximate throughput of 5×10^5 beads s^{-1} .

Buffer medium exchange

The buffer exchange system was initially evaluated in a reference experiment using only EB coloured buffer and a pure cross-flow wash buffer. The concentration of EB was monitored at the chip outlet while the cross-flows of four junctions were sequentially activated, each providing a buffer exchange of 25% of the $80 \mu\text{L min}^{-1}$ main flow. As can be seen in Figs. 4 and 5, the sequential buffer exchange provided an approximate decrease of dye content of 25% for each of the four cross-flow junctions. After the fourth junction about 3% EB remained which can be attributed to diffusion across the laminar boundaries and/or minor

Fig. 5 Composite image of the flow near each of the first four junctions along the main channel. At each junction 25% of a buffer containing blue dye (EB) is removed on one side of the channel, while supplying the same amount of colourless buffer on the opposing side

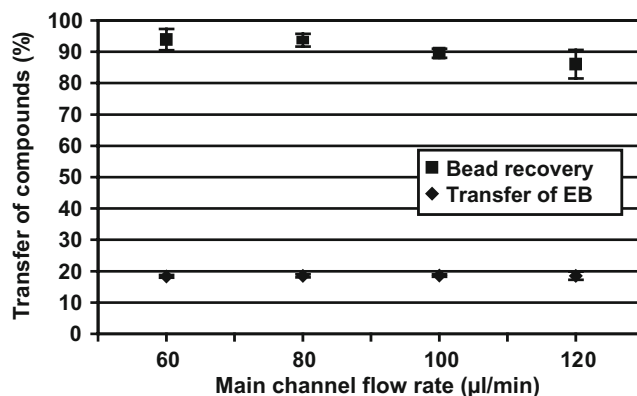
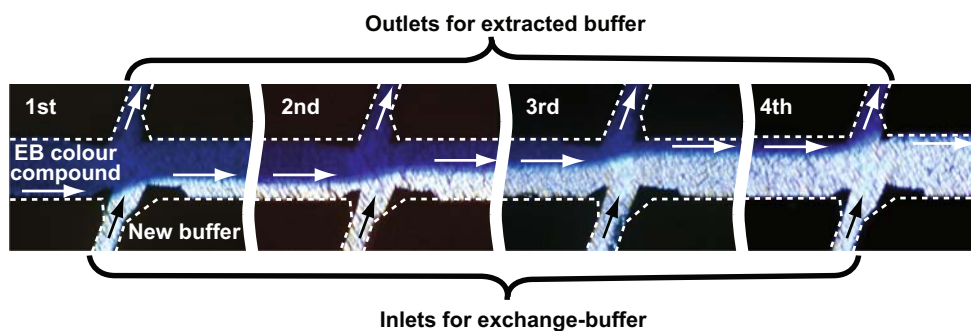


Fig. 6 Transfer of EB and beads after wash in the device for different flow rates are shown, when using four cross-flow junctions, each having an exchange rate of 25% of the main flow. Solid content, ~2%; input bead number, $\sim 500 \times 10^6 \text{ mL}^{-1}$. $N=4$ for all measurement points

disturbances in the flow. To investigate if acoustic streaming [28] played a role in mixing fluids across their laminar boundaries when actuating the system with ultrasound, the reference experiment described above was also performed using four cross-flow junctions with a theoretical buffer exchange of 100%. As can be seen in Fig. 4 (100% US), it was noted that the EB carry-over increased to 4% as the ultrasonic actuation was activated, as compared to 3% without ultrasound.

Particle washing

In a first set of experiments using microparticles, bead suspensions containing EB dye were washed in the device by using four consecutive cross-flow junctions each exchanging 25% of the volume flow of that in the main channel, theoretically exchanging a total of 100% of the volume flow. The main flow was varied from 60 to $120 \mu\text{L min}^{-1}$ while preserving the relative exchange rate of 25% in all of the side flows. Visual surveillance of the process confirmed that a band of particles was forming in the centre of the acoustically active segments in accordance with the acoustic radiation force theory. It was observed that variation of the flow rate in the channel had no effect on the removal of EB but that the recovery of beads decreases with

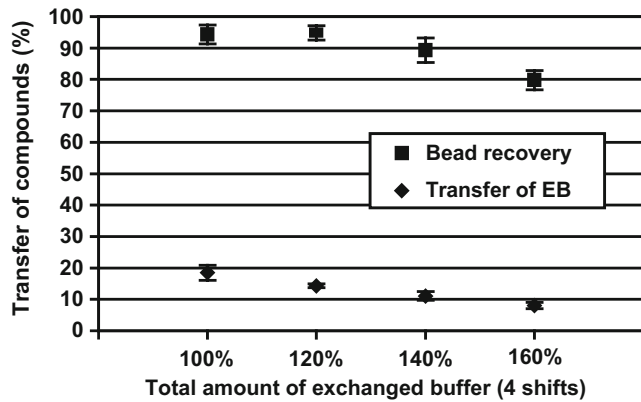


Fig. 7 Transfer of EB and beads when varying the exchange rate of the cross-flow junctions, when using four shifts and a main flow rate of $80 \mu\text{L min}^{-1}$. The solid content was $\sim 2\%$ and the input bead number was $\sim 500 \times 10^6 \text{ mL}^{-1}$. $N = 6$ for all measurement points

increasing flow rate. This is expected as an increased flow rate yields a shorter retention time for the particles in the 6 mm acoustic zone after each cross-flow junction and thus, above a given flow rate (break point), particles will not be refocused to the channel centre before reaching the subsequent cross-flow junction. Thereby non-focused particles will sequentially be lost at each junction. It can be seen in Fig. 6 that the break point in flow rate for a significant loss of particles occurs between 80 and $100 \mu\text{L min}^{-1}$.

At a main flow rate of $80 \mu\text{L min}^{-1}$ the recovery of beads was 94% of the input number while the transfer of EB was 19% of the input concentration (Fig. 6). This result is similar to what was reported by Peterson et al. [24] for a bead and dye mixture when using comparable flow conditions i.e. when performing an intended buffer exchange of 100%.

Increasing the relative exchange rate to 40% in each of four consecutive junctions, with a particle suspension input

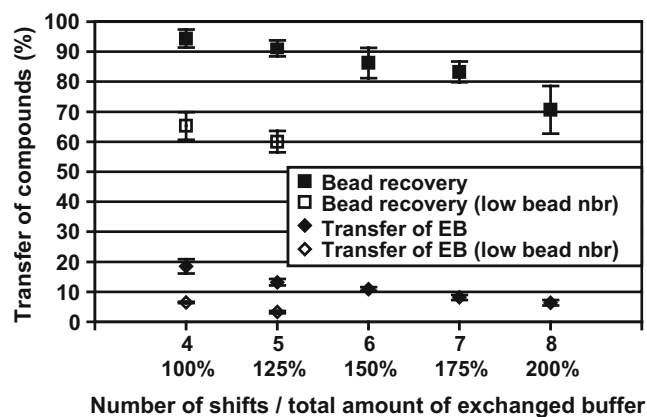


Fig. 8 Transfer of EB and beads when varying the number of cross-flows. Each cross-flow was set to 25% of the $80 \mu\text{L min}^{-1}$ main channel flow. The solid content was $\sim 2\%$ and the input bead number was $\sim 500 \times 10^6 \text{ mL}^{-1}$. Data for $\sim 0.2\%$ solid content (denoted low bead concentration) also shown. $N = 5$ for all measurement points

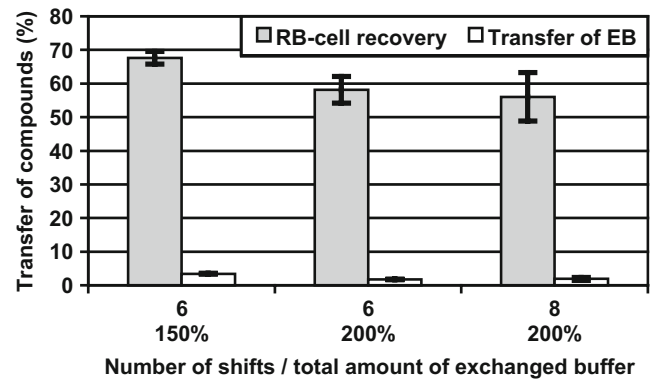


Fig. 9 Transfer of EB and recovery of erythrocytes for three different flow configurations. Main flow rate was set to $50 \mu\text{L min}^{-1}$. The haematocrit of the input sample was $\sim 2\%$. $N = 3$ for all bars

flow of $80 \mu\text{L min}^{-1}$, improved the washing performance to an 8% transfer of EB while recovering 80% of the beads (Fig. 7).

A higher number of fluid exchange junctions can also be employed to improve the washing performance. The buffer exchange efficiency for four to eight consecutive cross-flow junctions was evaluated when exchanging 25% in each cross-flow junction at an $80 \mu\text{L min}^{-1}$ particle suspension input flow rate (Fig. 8). Notably the loss of beads is all together 6% in the first four junctions while being 3–10% for each junction for higher numbers of junctions. This is attributed to the fact that the amplitude in the ultrasonic standing wave field decreases with the distance from the ultrasonic source, and thus full refocusing of particles to the channel centre was not accomplished after junctions 5 to 8. The location of the piezoceramic actuator to the vicinity of the prefocusing segment (Fig. 1) also supports this.

A rather drastic improvement in EB removal was observed when reducing the input bead content from 2 vol.% ($\sim 500 \times 10^6 \text{ mL}^{-1}$) to 0.2 vol.% ($\sim 50 \times 10^6 \text{ mL}^{-1}$). Using five consecutive junctions, each exchanging 25% of the $80 \mu\text{L min}^{-1}$ main flow, the EB content in the washed samples was reduced to 3.2% of the input concentration (compare this to 13% for higher bead content). The recovery of beads was only 60% for lower bead numbers (Fig. 8). However, by decreasing the main flow rate, a bead recovery of 74% and 3.6% EB transfer was achieved for five consecutive junctions.

Erythrocyte washing

To investigate the applicability of the system for cell handling purposes a mixture of human red blood cells and EB dye in PBS was prepared. The cells were successfully handled in the device, recovering 58% of the cells and reducing the EB content to 1.7% after wash. Two alternative flow setups were tested both having a main

flow of $50 \mu\text{L min}^{-1}$. In the first setup all of the eight consecutive junctions were used each exchanging 25% of the buffer in the main channel. In the second configuration six junctions were used, each exchanging 33% of the main channel buffer volume. It was noted that a 33% cross-flow in six consecutive junctions yielded almost the same cell and EB transfer through the device as the set-up with 25% cross-flow in eight consecutive junctions. In both cases a total of 200% of the main flow volume was exchanged. Figure 9 shows the obtained erythrocyte data.

Discussion

The washing performance of the device is strongly related to the total amount of exchanged medium. To improve the performance of the device an effort should be directed towards minimizing the bead loss by creating a more uniform force field along the channel. This would allow for a high exchange rate in all of the individual flow junctions, increasing the washing performance, and thus minimizing the number of active junctions. High bead levels in the processed samples have a negative influence on the washing performance suggesting that the device is more suited for applications such as analytical sample preparation or bead based affinity extraction rather than for processing dense cell suspensions. This limitation was also reported by Hawkes et al. [16] and Peterson et al. [17] for yeast cells and polyamide beads, respectively.

The higher bead recovery for richer bead suspensions may be caused by the fact that particles focused in the pre focusing segment could display a reduced overall Stokes drag as the beads move in a tight formation (as a fixed fluid) rather than as individual particles. On the contrary this tight particle band formation may also hydrodynamically encapsulate liquid containing dissolved species, which reduces the wash efficiency. This can be explained by the fact that a dense particle formation will display a resistance to perfusion by the wash buffer as it traverses the flow channel, consequently causing a lowered wash efficiency as compared to a dilute particle suspension. It should also be commented that diffusion over

laminar boundaries as well as compounds associated to the bead surface will further add to the carry-over.

The relatively high level of remaining EB (19%) in the particle wash experiment in Fig. 6 where 100% buffer exchange is performed via 4 cross-flow junctions is explained to be linked to the dye molecules being weakly adsorbed to the micro bead surface. Thus the total surface area available is a determinant for the accomplished wash efficiency. This is well supported by the fact that the wash efficiency is vastly improved for identical buffer exchange conditions when the solid content of the suspension is reduced from 2% to 0.2%.

Other means of addressing the wash efficiency is to exchange the carrier buffer more than 100% as is shown in Fig. 7 where the cross-flow rate is increased from 25% to 40% using only four cross-flow junctions and the transfer of EB is reduced from 19% to 8%. It should be pointed out that this is accomplished on account of a slightly increased loss in microbeads. Optionally, improved wash efficiency can be accomplished by increasing the number of cross-flow junctions as demonstrated in Fig. 8 where the EB transfer is reduced from 19% using four junctions to 6% using eight junctions.

It was also noted that the size distribution of the washed bead suspensions were biased towards larger diameters, i.e. smaller particles were to a larger extent extracted with the waste flow compared to the larger particles. This is explained by the fact that smaller particles move slower in the acoustic standing wave field than the larger particles as the velocity scales with the square of the diameter, Eq. 4. Hence smaller particles do not have sufficient time to refocus in the channel centre and reach a flow path sufficiently distant from the side channel waste outlets after each cross-flow junction.

In regards to performing cell manipulation using ultrasonic standing wave fields, concerns are frequently raised regarding the compatibility of ultrasonic manipulation and the impact of ultrasound on cells. Several studies have proven that ultrasonic cell manipulation in acoustic standing wave fields is not inducing any monitorable damage to the cells. Specifically, studies on the effects of ultrasonic trapping and in-chip culturing of yeast cells have recently

Table 1 Comparison of throughput and washing efficiency for three chip-integrated continuous flow based methods

Method	Flow rate ($\mu\text{L min}^{-1}$)	Beads/cells (s^{-1})	Bead/cell conc. (mL^{-1})	Transfer of contaminant (%)	Reference
Acoustophoresis	80	$\sim 5 \times 10^4$	$\sim 5 \times 10^7$	~ 3	This paper
Hydrodynamic filtration	60	$\sim 1 \times 10^3$	$\sim 1 \times 10^6$	No data ^a	[11]
Hydrodynamic filtration	<1	No data	No data	~ 1.5	[12]
Dielectrophoresis	2.5	$\sim 5 \times 10^2$	$\sim 1 \times 10^6$	No data ^b	[8]
Dielectrophoresis	0.15	No data	No data	~ 40	[9]

^a Contaminant transfer was $\sim 0\%$ for a particle free system.

^b The publication did not address transfer of molecular species.

been demonstrated [29]. It has also been established that acoustic microchip separation methods are gentle to erythrocytes and do not induce haemolysis [30] or significant release of intracellular components [31]. It has also been shown that cells proliferate at an unperturbed rate after being exposed to an acoustic standing wave field [32–34].

Compared to other chip-integrated continuous flow based methods for buffer exchange, the particle concentration and volumetric throughput in acoustophoresis systems is rather high as compared to dielectrophoresis and hydrodynamic filtration as reported in the literature (Table 1). A basic requirement for efficient buffer exchange is the ability to move beads or cells significantly faster than the diffusion rate of the molecular species in the suspension. It should also be noted that high concentrations of particulate matter is likely to be limiting the washing efficiency for any continuous flow chip-based process since a perturbation of the flow path is inherent with the transversal movement of the beads or cells.

Conclusions

The presented ultrasonically controlled cross-flow buffer exchange strategy offers a continuous flow methodology for tuneable on-line particle and cell washing. The particle wash chip demonstrated a carry-over of molecular material, EB, down to 3.2% for micro beads and 1.7% for erythrocytes using an eight cross-flow channel configuration. The wash efficiency competes well with previously presented devices for continuous washing of particulate matter in microfluidic systems, demonstrating a higher process capacity in terms of cell throughput and input particle/cell concentration. Although being on an early stage of development, the proposed buffer exchange strategy, utilising repetitive acoustic wash cycles, has the potential to be a tool for cell handling and bead based affinity extraction applications performed in a continuous flow through format. The design principle also supports multiple buffer exchange sequences for cells or beads during one passage through the device, which can be desirable for e.g. preparation of functionalized bead suspensions or for in line staining or stimulation of cells.

Acknowledgement The authors would like to thank the Carl Trygger Foundation, the Crafoord Foundation, the Swedish Research Council and Vinnova for funding.

References

- Dai BA, Wang L, Djaiani G, Mazer CD (2004) Continuous and discontinuous cell-washing autotransfusion systems. *J Cardiothorac Vasc Anesth* 18:210
- Ekström S, Malmström J, Wallman L, Löfgren M, Nilsson J, Laurell T, Marko-Varga G (2002) On-chip microextraction for proteomic sample preparation of in-gel digests. *Proteomics* 2:413
- Maniatis T, Fritsch EF, Sambrook J (1989) *Molecular cloning: a laboratory manual*. Cold Spring Harbor Laboratory Press, New York
- Whitesides GM (2006) The origins and the future of microfluidics. *Nature* 442:368
- Pamme N (2007) Continuous flow separations in microfluidic devices. *Lab Chip* 7:1644
- Molloy JE, Padgett MJ (2002) Lights, action: optical tweezers. *Contemp Phys* 43:241
- MacDonald MP, Spalding GC, Dholakia K (2003) Microfluidic sorting in an optical lattice. *Nature* 426:421
- Besette PH, Hu XY, Soh HT, Daugherty PS (2007) Microfluidic library screening for mapping antibody epitopes. *Anal Chem* 79:2174
- Tornay RL, Braschler T, Demierre N, Steitz B, Finka A, Hofmann H, Hubbell JA, Renaud P (2008) Dielectrophoresis-based particle exchanger for the manipulation and surface functionalization of particles. *Lab Chip* 8:267
- Peyman SA, Iles A, Pamme N (2008) Rapid on-chip multi-step (bio)chemical procedures in continuous flow—manoeuvring particles through co-laminar reagent streams. *Chem Commun* (10):1220–1222
- Yamada M, Kobayashi J, Yamato M, Seki M, Okano T (2008) Millisecond treatment of cells using microfluidic devices via two-step carrier-medium exchange. *Lab Chip* 8:772
- VanDelinder V, Groisman A (2007) Perfusion in microfluidic cross-flow: separation of white blood cells from whole blood and exchange of medium in a continuous flow. *Anal Chem* 79:2023
- Harris N, Hill M, Shen Y, Townsend RJ, Beeby S, White N (2004) A dual frequency, ultrasonic, microengineered particle manipulator. *Ultrasonics* 42:139
- Nilsson A, Petersson F, Jönsson H, Laurell T (2004) Acoustic control of suspended particles in micro fluidic chips. *Lab Chip* 4:131
- Harris NR, Hill M, Beeby S, Shen Y, White NM, Hawkes JJ, Coakley WT (2003) A silicon microfluidic ultrasonic separator. *Sens Actuators B Chem* 95:425
- Hawkes JJ, Barber RW, Emerson DR, Coakley WT (2004) Continuous cell washing and mixing driven by an ultrasound standing wave within a microfluidic channel. *Lab Chip* 4:446
- Petersson F, Nilsson A, Jönsson H, Laurell T (2005) Carrier medium exchange through ultrasonic particle switching in microfluidic channels. *Anal Chem* 77:1216
- Laurell T, Petersson F, Nilsson A (2007) Chip integrated strategies for acoustic separation and manipulation of cells and particles. *Chem Soc Rev* 36:492
- Gorkov LP (1962) On the forces acting on a small particle in an acoustical field in an ideal fluid. *Sov Phys Doklady* 6:773
- Yosioka K, Kawasima Y (1955) Acoustic radiation pressure on a compressible sphere. *Acustica* 5:167
- Weiser MAH, Apfel RE, Neppiras EA (1984) Interparticle forces on red-cells in a standing wave field. *Acustica* 56:114
- Woodside SM, Bowen BD, Piret JM (1997) Measurement of ultrasonic forces for particle–liquid separations. *AIChE J* 43:1727
- Hawkes JJ, Coakley WT (2001) Force field particle filter, combining ultrasound standing waves and laminar flow. *Sens Actuators B Chem* 75:213
- Petersson F, Nilsson A, Holm C, Jönsson H, Laurell T (2005) Continuous separation of lipid particles from erythrocytes by means of laminar flow and acoustic standing wave forces. *Lab Chip* 5:20
- Yasuda K, Kamakura T (1997) Acoustic radiation force on micrometer-size particles. *Appl Phys Lett* 71:1771
- Kapishnikov S, Kantsler V, Steinberg V (2006) Continuous particle size separation and size sorting using ultrasound in a

- microchannel. *J Stat Mech* 2006:P01012 doi:[10.1088/1742-5468/2006/01/P01012](https://doi.org/10.1088/1742-5468/2006/01/P01012)
27. Petersson F, Åberg L, Swärd-Nilsson AM, Laurell T (2007) Free flow acoustophoresis: microfluidic-based mode of particle and cell separation. *Anal Chem* 79:5117
 28. Bengtsson M, Laurell T (2004) Ultrasonic agitation in microchannels. *Anal Bioanal Chem* 378:1716
 29. Evander M, Johansson L, Lilliehöj T, Piskur J, Lindvall M, Johansson S, Almqvist M, Laurell T, Nilsson J (2007) Noninvasive acoustic cell trapping in a microfluidic perfusion system for online bioassays. *Anal Chem* 79:2984
 30. Jönsson H, Holm C, Nilsson A, Petersson F, Johnsson P, Laurell T (2004) Particle separation using ultrasound can radically reduce embolic load to brain after cardiac surgery. *Ann Thorac Surg* 78:1572
 31. Yasuda K, Haupt SS, Umemura S, Yagi T, Nishida M, Shibata Y (1997) Using acoustic radiation force as a concentration method for erythrocytes. *J Acoust Soc Am* 102:642
 32. Hultström J, Manneberg O, Dopf K, Hertz HM, Brismar H, Wiklund M (2007) Proliferation and viability of adherent cells manipulated by standing-wave ultrasound in a microfluidic chip. *Ultrasound Med Biol* 33:145
 33. Pui PWS, Trampler F, Sonderhoff SA, Groeschl M, Kilburn DG, Piret JM (1995) Batch and semicontinuous aggregation and sedimentation of hybridoma cells by acoustic-resonance fields. *Biotechnol Prog* 11:146
 34. Radel S, McLoughlin AJ, Gherardini L, Doblhoff-Dier O, Benes E (2000) Viability of yeast cells in well controlled propagating and standing ultrasonic plane waves. *Ultrasonics* 38:633